Original Article

PMP
Progress in Medical Physics 29(2), June 2018
https://doi.org/10.14316/pmp.2018.29.2.47
eISSN 2508-4453

Effect of Low Magnetic Field on Dose Distribution in the SABR Plans for Liver Cancer

Jaeman Son*, Minsoo Chun*, Hyun Joon An*, Seong-Hee Kang†, Eui Kyu Chie*,†,§,‖, Jeongmin Yoon*, Chang Heon Choi*, Jong Min Park*,†,§,¶, Jung-in Kim*,†,§

*Department of Radiation Oncology, Seoul National University Hospital, Seoul, †Department of Radiation Oncology, Seoul National University Bundang Hospital, Seongnam, ‡Biomedical Research Institute, Seoul National University Hospital, §Institute of Radiation Medicine, Seoul National University Medical Research Center, ‖Department of Radiation Oncology, Seoul National University College of Medicine, Seoul, ¶Center for Convergence Research on Robotics, Advanced Institutes of Convergence Technology, Suwon, Korea

Received 24 May 2018
Revised 20 June 2018
Accepted 21 June 2018

Corresponding author
Jung-in Kim
(madangin@gmail.com)
Tel: 82-2-2072-3573
Fax: 82-2-765-3317

To investigate the effect of low magnetic field on dose distribution in SABR plans for liver cancer, we calculated and evaluated the dose distribution to each organ with and without magnetic fields. Ten patients received a 50 Gy dose in five fractions using the ViewRay® treatment planning system. For planning target volume (PTV), the results were analyzed in the point minimum (D_{min}), maximum (D_{max}), mean dose (D_{mean}) and volume receiving at least 90% ($V_{90\%}$), 95% ($V_{95\%}$), and 100% ($V_{100\%}$) of the prescription dose, respectively. For organs at risk (OARs), the duodenum and stomach were analyzed with $D_{0.5cc}$ and D_{2cc}, and the remained liver except for PTV was analyzed with D_{mean}, D_{max}, and D_{min}. Both inner and outer shells were analyzed with the point D_{min}, D_{max}, and D_{mean}, respectively. For PTV, the maximum change in volume due to the presence or absence of the low magnetic field showed a percentage difference of up to 0.67±0.60%. In OAR analysis, there is no significant difference for the magnetic field. In both shell structure analyses, although there are no major changes in dose distribution, the largest value of deviation for D_{max} in the outer shell is 2.12±2.67 Gy. The effect of low magnetic field on dose distribution by a Co-60 beam was not significantly observed within the body, but the dose deposition was only appreciable outside the body.

Keywords: Liver cancer, SABR, MR-IGRT, Magnetic field

Introduction

Primary liver cancer represented 782,500 new liver cancer cases in 2012.[1] In general, surgery is preferred in patients with hepatocellular carcinoma (liver cancer), but surgery may be difficult depending on the location of the tumor or the history of the patient. In this case, it is known that external beam radiation therapy (EBRT) is helpful for local control. Among the various EBRT techniques, Stereotactic ablative radiotherapy (SABR) is commonly used for liver cancer. In contrast to conventional radiotherapy, which delivers low dose to a larger volume for a higher number of daily fractions, SABR is usually given as a single dose or up to five doses once a day with tumor ablation and maximal normal-tissue sparing.[2-6] Despite these advantages, it could lead a more severe damage compared to conventional therapy if the positioning error occurred. Therefore, the very high dose such as SABR must entail with one or more sessions of treatment planning with computed tomography (CT) or other advanced imaging

techniques to precisely and accurately map the position of the tumor due to high dose radiation. Hence, a commercial MR-IGRT system (ViewRay®, ViewRay Inc., Cleveland, OH, USA) has been recently developed in the clinic. An onboard MR imaging system of ViewRay® was developed with 0.35 T low magnetic field and a radiation therapy system was developed with three cobalt-60 radiotherapy sources.[7-9] Although the use of MRI can be a more accurate and precise treatment, a localized region of dose enhancement and dose reduction effects can be caused by magnetic field in ViewRay®. In other words, the geometric of this system results in perturbation on dose distribution, such as changes to the percentage depth dose, tissue interface effects and lateral shifts in dose distributions in the photon beam radiotherapy. Thus, the effects of magnetic field changes on dose distribution for radiotherapy treatment have been studied by many groups through various techniques including analytical, simulation and/or experimental.[10-12] Raaijmakers et al. reported that the magnetic field strength will cause dose enhancement at tissue-air boundaries, due to the electron return effect (ERE). ERE is that electrons entering air will describe a circular path and return into the phantom causing extra dose deposition. In this paper, ERE causes a dose enhancement of 40% at the beam exit area of the phantom.[13] In 2007, they also reported on the correlation between magnetic field and dose enhancement or dose reduction.[14] In addition, Kim et al.[15] investigated the effect of low magnetic field on dose distribution and reported that low magnetic field has not significantly effects on dose distribution in body for partial breast irradiation (PBI). On the base of this results, the aim of this work was to clinically evaluate the effects of low magnetic field on dose distributions. It was performed with and without low magnetic field (0.35 T) in SABR plans for liver cancer.

Materials and Methods

1. Patient selection

Ten patients, treated with SABR techniques delivered 50 Gy in 5 fractions using ViewRay® system for liver cancer from October 2015 to April 2018, were selected.

2. Treatment planning in ViewRay® system

Intensity-modulated radiotherapy (IMRT) plans for liver cancer were used with SABR using the ViewRay® system. The ViewRay® treatment planning system (TPS) modelled using its own novel optimization algorithm and dose calculation based on Monte Carlo (MC) algorithm. The ViewRay® system consists of a rotating gantry with tree Co-60 heads spaced 120° apart that can generate a maximum dose rate of 550 cGy/min at the isocenter. The MLC of ViewRay® is the only beam-shaping device in the beam path when the Co-60 source is at Beam On position. Each MLC consists of 60 double-focused MLC mounted on two opposed leaf banks (30 leaf-pairs) to minimize the penumbra. The leaf width is 1.05 cm at isocenter of 105 cm (covering a square field of 27.3×27.3 cm^2). The average size of the PTV is 46.82±38.67 cm^3 (8.3–152 cm^3). Several organs at risk (OAR) were contoured: duodenum, stomach and remained normal liver. To investigate the effect for magnetic field in boundary between air and medium, two shell structures close to the body outline of the patients were generated on dose distribution, this method was verified in the paper of Kim et al.[15] Two shell structures, consist of inner shell and outer shell, were ±0.3 cm thickness centrally the body surface. The thickness takes into account all of dose grid and common margin used in our institution. In this study, the IMRT efficiency and level was set at the value of 1.0 and 3.0, respectively. The parameter of efficiency is for optimization of a relatively smoother fluence map and the parameter of level is for discretization of each fluence map. The resolution of dose grid was set at of 0.3 cm. Each of the SABR plans for liver cancer were applied with both options for dose calculation with magnetic field and zero magnetic field.

3. Dosimetric parameter analysis

To investigate these dose differences with and without magnetic field, we compared the results of dose distribution for the case of liver cancer patient with and without magnetic field based on Dose volume histograms (DVHs). All results were analyzed from the DVHs of each patient to obtain values at each dose and volume with and without low magnetic field. For PTV, the dose analyzed at the point

minimum (D_{min}), maximum (D_{max}), mean dose (D_{mean}) and volume receiving at least 90% ($V_{90\%}$), 95% ($V_{95\%}$) and 100% ($V_{100\%}$) of the prescribed dose, respectively. For OARs, the duodenum was analyzed the dose receiving 0.5 cc ($D_{0.5cc}$) and 2 cc (D_{2cc}) of total duodenum volume, and the results of stomach were analyzed under the same conditions of duodenum. In addition, we defined the liver dose constraints that at least 700 mL of the normal liver volume (total liver volume minus PTV) should be received 21 Gy or less. Both inner and outer shells were analyzed with the D_{min}, D_{max}, and D_{means}, respectively.

Results

The comparison of dose distributions for the case of liver cancer patient with and without magnetic field was shown in Fig. 1. The magnetic field was applied to perform the calculation of a dose distribution with magnetic field. In addition, we analyzed the results of the dosimetric parameter for different structure.

1. The effect of low magnetic field in PTV

The dose distribution changes in PTV were calculated with and without magnetic field. The average difference of mean dose values was 0.07±0.05 Gy, and the maximum difference was 0.19 Gy and the minimum difference was 0.03 Gy. For the point dose analysis, the average differences of D_{min} and D_{max} were 0.28±0.33 Gy and 0.30±0.25 Gy, respectively. The average difference of $V_{90\%}$, $V_{95\%}$, and $V_{100\%}$ for volumes of PTV shows no significant difference. However, these results were indicated for the average difference value. The maximum difference of $V_{100\%}$ showed 1.77%, which a slight difference was showed. Fig. 2 shows the difference dose and volume for ten patients in the PTV dose-volume

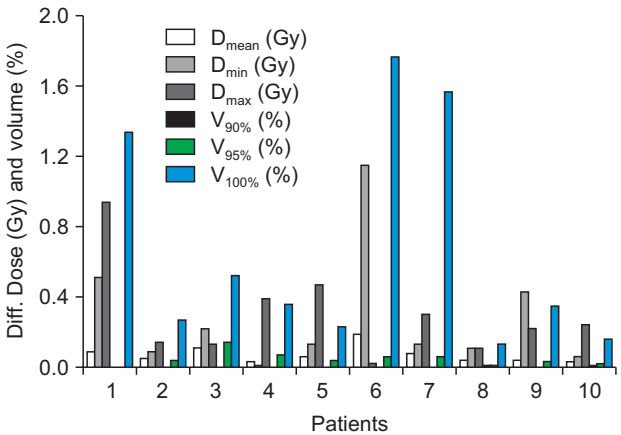

Fig. 2. Dose and volume difference values in PTV for each patient.

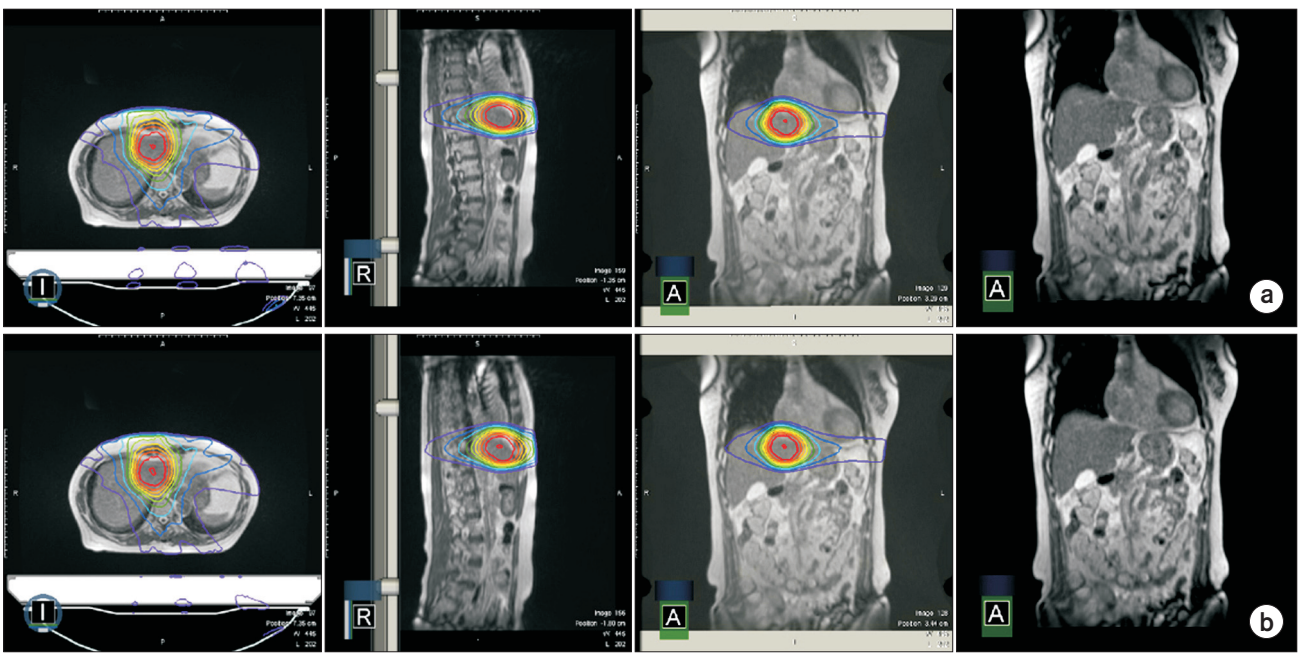

Fig. 1. The comparison of dose distribution (a) with magnet and (b) without magnet field in the case of liver SABR with a magnet field (B_0).

analysis. Table 1 analyzed the result of the average dose volume difference for PTV.

2. The effect of low magnetic field in OARs

Table 2 shows the analysis of the average dose volume difference for OARs including duodenum, stomach and remained normal liver. The average differences of the $D_{0.5cc}$ and were 0.05±0.05 Gy and 0.06±0.04 Gy in duodenum, respectively. In the stomach analysis, the average differences of $D_{0.5cc}$ and D_{2cc} were 0.31±0.69 Gy and 0.12±0.18 Gy, respectively. In the remained normal liver, the average differences of D_{mean} and D_{min} showed no significant difference. The average difference of the D_{max} was 0.33±0.36 Gy in the remained normal liver. In these OARs analysis, there were no significant differences.

Table 1. The average dosimetric parameter analysis for PTV.

Analysis	With Magnet	Without Magnet	Difference value	*P*-value
D_{mean} (Gy)	52.42±1.19	52.44±1.15	0.07±0.05	0.22
D_{max} (Gy)	55.99±2.43	55.89±2.20	0.30±0.25	0.31
D_{min} (Gy)	45.98±1.11	46.05±1.19	0.28±0.33	0.21
$V_{90\%}$ (%)	99.99±0.04	99.99±0.04	0.00±0.00	0.50
$V_{95\%}$ (%)	99.65±0.29	99.66±0.30	0.05±0.04	0.26
$V_{100\%}$ (%)	90.54±8.07	90.64±7.77	0.67±0.60	0.37

3. The effect of low magnetic field near the body surface

Table 3 analyzed the result of the average dose difference for shell structures. For inner shell and outer shell, the average dose difference of mean dose values was 0.02±0.02 Gy and 0.08±0.07 Gy, which there is no dose difference with and without magnetic field. For dose minimum of point dose, there is also no dose difference for inner shell and outer shell. In inner shell, the average difference of dose maximum was 0.59±0.92 Gy, the maximum difference was 3.15 Gy with and without magnetic field. In outer shell, the average difference of dose maximum was 2.12±2.67 Gy, the maximum difference was 4.38 Gy with and without mag-

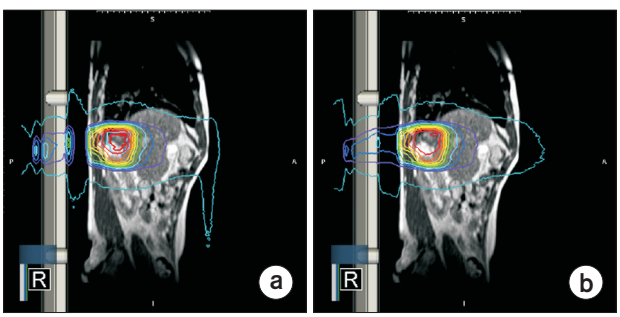

Fig. 3. The dose distribution in sagittal image between (a) with magnet field (B_0) and (b) without magnet field.

Table 2. The average dosimetric parameter analysis for organs at risk (OARs).

OARs	Analysis	With Magnet	Without Magnet	Difference value	*P*-value
Duodenum	$D_{0.5cc}$ (Gy)	7.01±7.93	7.00±7.92	0.05±0.05	0.40
	D_{2cc} (Gy)	5.23±5.24	5.25±5.25	0.06±0.04	0.29
Stomach	$D_{0.5cc}$ (Gy)	12.81±7.26	12.56±7.53	0.31±0.69	0.19
	D_{2cc} (Gy)	11.35±6.78	11.28±6.87	0.12±0.18	0.18
Remained normal liver	D_{mean} (Gy)	11.12±2.53	11.13±2.54	0.01±0.01	0.16
	D_{max} (Gy)	52.46±1.70	52.32±1.55	0.33±0.36	0.16
	D_{min} (Gy)	0.50±0.21	0.48±0.19	0.03±0.03	0.19

Table 3. The average dosimetric parameter analysis for shell structures.

	Analysis	With Magnet	Without Magnet	Difference value	*P*-value
Inner shell	D_{mean} (Gy)	1.34±0.53	1.35±0.52	0.02±0.02	0.21
	D_{max} (Gy)	31.49±4.82	31.97±4.78	0.59±0.92	0.09
	D_{min} (Gy)	0.02±0.01	0.02±0.01	0.00±0.00	0.50
Outer shell	D_{mean} (Gy)	1.00±0.38	0.98±0.34	0.08±0.07	0.34
	D_{max} (Gy)	21.14±3.75	22.29±4.07	2.12±2.67	0.16
	D_{min} (Gy)	0.02±0.01	0.02±0.01	0.00±0.00	0.30

netic field, which the dose difference was greater in outer shell than in inner shell. Fig. 3 shows the dose distribution in sagittal images between with and without magnetic field. A magnetic field transverse to the beam direction shows dose deposition outside the body, because the secondary electrons scattered from the body and produced in the treatment head travel in the direction of the magnetic field.

Discussion

Two methods, MC dose computation algorithms with and without magnetic field, were used in the TPS of ViewRay®. To perform a highly optimized simulation of the photons using a variety of variance reduction techniques, both MC algorithms apply the same techniques. The MC algorithm without the magnetic field tracks and calculates only the photons using the geometry information of patient without considering the magnetic field. However, MC algorithm with a magnetic field calculates while tracking charged particles including the effect of the magnetic field. Secondary electrons a photon produces move in a predominantly forward direction and travel in a series of a helical trajectory when calculating without magnetic field. When a photon beam irradiates with a magnetic field, charged particles are deflected by the Lorentz force. The path of these particles is the series of arc-shaped trajectories in tissue or water, not a helical trajectory. This phenomenon is called the tissue interface effects (equal to ERE) by Raaymaker et al. These results indicate that the magnetic field can affect the change of the dose distribution. In addition, they extended to the more general case with angulated air-tissue boundaries in 2007.[14] Although the effects of ERE counteract as using opposing beam, dose increase or decrease of respectively up to 7 and 12% occur in the region near the tilted surface. A.D. Esmaeeli et al. clinically studied that the consequences to radiation dose distributions were occurred in different magnetic field strengths for breast plans.[16] The paper reported that the magnetic field have an effect on dose distribution in the internal and contralateral tissues and increase it to the PTV with sharper edge DVH curve. In our study, however, the effect of magnetic field on the dose distribution of internal tissues and PTV can be neglected. That of outside the body can only have a significant increasing dose. These results are different that's because relatively low magnetic field of 0.35 T set up the relatively small Lorentz force. Besides, the large uncertainty for dose and volume was included in the results obtained in this study due to small number of samples and large dose grid thickness. Further studies are necessary to investigate the effect of magnetic field on dose distribution based on various treatment sites, techniques and cases.

Conclusion

The effect of the low magnetic field on dose distribution was not significantly observed PTV and OARs for SABR plans with liver cancer. The dose distribution change with and without low magnetic field was only appreciable outside the body, and there was no significant difference in PTV, OARs and inner shell.

Acknowledgements

This work was supported by the National Research Foundation of Korea (NRF) grant funded by the Korea government (MSIP) (No.NRF-2017M2A2A7A02020643, No.NRF-2017M2A2A7A02020641).

Conflicts of Interest

The authors have nothing to disclose.

Availability of Data and Materials

All relevant data are within the paper and its Supporting Information files.

References

1. Torre LA, Bray F, Siegel RL, Ferlay J, Lortet-Tieulent J, Jemal A. Global cancer statistics, 2012. CA: a cancer journal for clinicians. 2015;65(2):87-108.
2. Huang K, Dahele M, Senan S, et al. Radiographic changes after lung stereotactic ablative radiotherapy (SABR)-can

we distinguish recurrence from fibrosis? A systematic review of the literature. Radiotherapy and Oncology. 2012; 102(3):335-42.
3. Finkelstein SE, Timmerman R, Mcbride WH, et al. The confluence of stereotactic ablative radiotherapy and tumor immunology. Clinical and Developmental Immunology. 2011;2011.
4. Myrehaug S, Sahgal A, Russo SM, et al. Stereotactic body radiotherapy for pancreatic cancer: recent progress and future directions. Expert review of anticancer therapy. 2016;16(5):523-30.
5. Pidikiti R, Stojadinovic S, Speiser M, et al. Dosimetric characterization of an image-guided stereotactic small animal irradiator. Physics in Medicine & Biology. 2011;56(8):2585.
6. Palma DA, Haasbeek CJ, Rodrigues GB, et al. Stereotactic ablative radiotherapy for comprehensive treatment of oligometastatic tumors (SABR-COMET): study protocol for a randomized phase II trial. BMC cancer. 2012;12(1):305.
7. Mutic S, Dempsey JF. The ViewRay system: Magnetic resonance-guided and controlled radiotherapy. Seminars in radiation oncology: Elsevier 2014:196-99.
8. Yang Y, Cao M, Sheng K, et al. Longitudinal diffusion MRI for treatment response assessment: Preliminary experience using an MRI-guided tri-cobalt 60 radiotherapy system. Medical physics. 2016;43(3):1369-73.
9. Wooten HO, Rodriguez V, Green O, et al. Benchmark IMRT evaluation of a Co-60 MRI-guided radiation therapy system. Radiotherapy and Oncology. 2015;114(3):402-5.
10. Burke B, Ghila A, Fallone B, Rathee S. Radiation induced current in the RF coils of integrated linac-MR systems: The effect of buildup and magnetic field. Medical physics. 2012;39(8):5004-14.
11. Rubinstein AE, Liao Z, Melancon AD, et al. A Monte Carlo study of magnetic-field-induced radiation dose effects in mice. Medical physics. 2015;42(9):5510-16.
12. Kirkby C, Stanescu T, Fallone B. Magnetic field effects on the energy deposition spectra of MV photon radiation. Physics in Medicine & Biology. 2008;54(2):243.
13. Raaijmakers AJ, Raaymakers BW, Lagendijk JJ. Integrating a MRI scanner with a 6 MV radiotherapy accelerator: dose increase at tissue-air interfaces in a lateral magnetic field due to returning electrons. Phys Med Biol. 2005;50(7):1363-76.
14. Raaijmakers AJ, Raaymakers BW, Van Der Meer S, Lagendijk JJ. Integrating a MRI scanner with a 6 MV radiotherapy accelerator: impact of the surface orientation on the entrance and exit dose due to the transverse magnetic field. Phys Med Biol. 2007;52(4):929-39.
15. Kim JI, Park SY, Lee YH, Shin KH, Wu H-G, Park JM. Effect of low magnetic field on dose distribution in the partial-breast irradiation. Progress in Medical Physics. 2015; 26(4):208-14.
16. Esmaeeli A, Pouladian M, Monfared A, Mahdavi S, Moslemi D. Effect of uniform magnetic field on dose distribution in the breast radiotherapy. International Journal of Radiation Research. 2014;12(2):161.